Transition Structure at the Si(100)-SiO_2 Interface

Angelo Bongiorno,[1,2] Alfredo Pasquarello,[1,2] Mark S. Hybertsen,[3] and L. C. Feldman[4]

[1]*Institut de Théorie des Phénomènes Physiques (ITP), Ecole Polytechnique Fédérale de Lausanne (EPFL), CH-1015 Lausanne, Switzerland*

[2]*Institut Romand de Recherche Numérique en Physique des Matériaux (IRRMA), CH-1015 Lausanne, Switzerland*

[3]*Agere Systems, 4 Connell Drive, Berkeley Heights, New Jersey 07922, USA*

[4]*Department of Physics and Astronomy, Vanderbilt University, Nashville, Tennessee 37235, USA*

(Received 5 September 2002; published 6 May 2003)

We characterize the transition structure at the Si(100)-SiO_2 interface by addressing the inverse ion-scattering problem. We achieve sensitivity to Si displacements at the interface by carrying out ion-scattering measurements in the channeling geometry for varying ion energies. To interpret our experimental results, we generate realistic atomic-scale models using a first-principles approach and carry out ion-scattering simulations based on classical interatomic potentials. Silicon displacements larger than 0.09 Å are found to propagate for three layers into the Si substrate, ruling out a transition structure with regularly ordered O bridges, as recently proposed.

DOI: 10.1103/PhysRevLett.90.186101 PACS numbers: 68.35.–p, 61.43.Bn, 61.85.+p, 68.49.–h

The gate oxide in Si-based electronic devices has been designed to be thinner with each new generation of the technology [1,2]. In the present generation, this oxide film has a thickness below 2 nm [3]. In this regime, the transition layer at the Si-SiO_2 interface constitutes a significant fraction of the total thickness and its detailed physical properties affect device performance [4]. The understanding of the Si-SiO_2 interface *at the atomic-scale* has proved to be very challenging and to be intimately coupled to understanding the mechanism of SiO_2 film growth.

Several experimental techniques [5–10] have so far provided well-defined atomic-scale information on the structure of the Si(100)-SiO_2 interface [11]. However, the bonding pattern connecting the Si substrate to the oxide remains to date poorly understood, as manifested by the variety of model structures in the recent literature [11–16]. Several recent models show a consensus in favoring transition structures in which the Si crystal remains essentially ideal and shows an ordered pattern of O bridges at the interface [14,15]. In an alternative model, the match between the Si crystal and its oxide occurs through a disordered Si layer [11,13]. These model structures reflect different assumptions concerning the oxidation mechanisms [13,15]. However, the transition structure near the interface cannot be distinguished by the available experimental data.

Ion-scattering experiments in the channeling geometry are particularly sensitive to the Si side of the Si-SiO_2 interface. From early measurements at a selected ion energy [17], the structure at the interface could be characterized in terms of *excess silicon yield* which mainly results from Si atoms out of register with respect to their ideal lattice positions. However, the interpretation of these data in terms of atomistic models is not trivial and requires the solution of the inverse scattering problem.

Here we combine ion-scattering experiments and theoretical modeling to investigate the nature of the atomic arrangements at the Si(100)-SiO_2 interface. In the ion-scattering experiments, we probed the extent of Si displacements close to the interface for varying ion energies. Our modeling approach aims at reproducing the observed yields for atomistic model structures complying with the available experimental data [6–9]. We generated such models by applying sequentially classical molecular dynamics and density-functional relaxation methods. By performing ion-scattering simulations on these model structures, we could address the inverse scattering problem and extract detailed information concerning the bonding in the vicinity of the Si(100)-SiO_2 interface.

Rutherford ion-scattering experiments were carried out at room temperature on oxides grown via a high quality rapid thermal oxidation process, known to produce device quality dielectric layers. Displaced Si atoms were detected by use of the channeling geometry [17,18]. The samples were oriented in a two axis goniometer and probed with a He^+ beam by incidence along the normal $\langle 100 \rangle$ direction. We used a grazing exit angle geometry with the detector at a scattering angle of approximately 95°. Absolute yields giving the amount of Si and O atoms were obtained with an estimated error of $\pm 5\%$.

We focus here on the excess Si yield [17], $\Delta Y = Y_{Si} - Y_O/2 - Y^{ideal}$, where Y_{Si} and Y_O are the Si and O yields, respectively, and Y^{ideal} the yield calculated for an ideally terminated Si crystal [18]. The excess Si yield is a genuine interface property, since the contribution from fully oxidized Si atoms ($Y_O/2$) and from the ideal Si crystal (Y^{ideal}) are subtracted out. Hence, ΔY results from Si atoms displaced out of their crystalline positions and from Si atoms in intermediate oxidation states. The latter contribution is only partially canceled by $Y_O/2$. In Fig. 1(a), we give measured ΔY for ion energies ranging

 © 2003 The American Physical Society

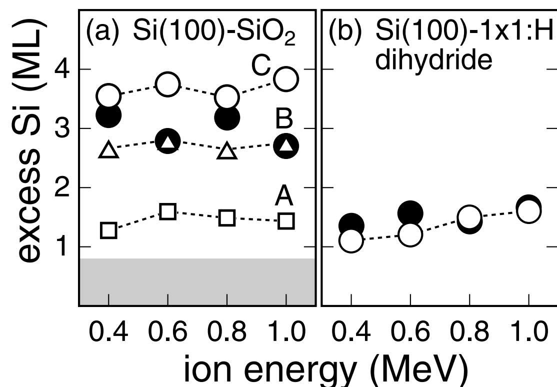

FIG. 1. Measured (full circles) and calculated excess Si yields vs ion energy for (a) the Si(100)-SiO_2 interface and (b) the Si(100)1×1:H surface. In (a), the calculated values are obtained for models *A* (squares), *B* (triangles), and *C* (circles); the contribution from partially oxidized Si atoms is shown by a shaded band. In (b), experimental values from Ref. [18].

between 0.4 and 1.0 MeV. In this regime, the measurement is sensitive to Si displacements between 0.09 and 0.14 Å [18].

We designed model interface structures to reproduce atomic-scale features consistent with various experimental probes [6–9]. After preparing a template consisting of a Si(100) surface with a particular bond pattern, classical molecular dynamics were used to evolve Si and O atoms at high temperatures in its neighborhood [19]. We used interatomic pair potentials of the Born-Mayer-Huggins type for which the parameters were derived from *ab initio* calculations [20]. A quench to low temperatures gave disordered SiO_2 oxides attached to the template, free of coordination defects. By removing O atoms, we could adjust the amount of Si atoms in intermediate oxidation states and their approximate location. The atomic positions were finally relaxed using a density-functional approach [21]. The interface models are periodic in the plane of the interface, with a $\sqrt{8} \times \sqrt{8}$ Si repeat unit. They consist of $\sim$12 Å of oxide at a density of 2.3 to 2.4 g/cm^3, in agreement with x-ray measurements [6]. We used 17 Si monolayers (MLs) for the substrate to achieve fully converged results in the ion-scattering simulations.

To match recent photoemission data [9], we considered three model interfaces all containing about 1.9 ML of Si atoms in intermediate oxidation states, distributed between Si^{+1}, Si^{+2}, and Si^{+3} as 1:1.7:2.3. However, the model interfaces differed considerably in their interfacial bonding at the Si termination (Fig. 2). In model *A*, the termination is nearly abrupt and closely corresponds to that of an ideal Si lattice. The bond density mismatch at the interface is accommodated by O bridges. The structure shows a slight departure from the ordered *stripe* phase [15] to accommodate the intermediate oxidation states [9]. The terminating Si layer contains 3 Si^{+1} and 5 Si^{+2} moieties per unit cell. The 7 Si^{+3} moieties are

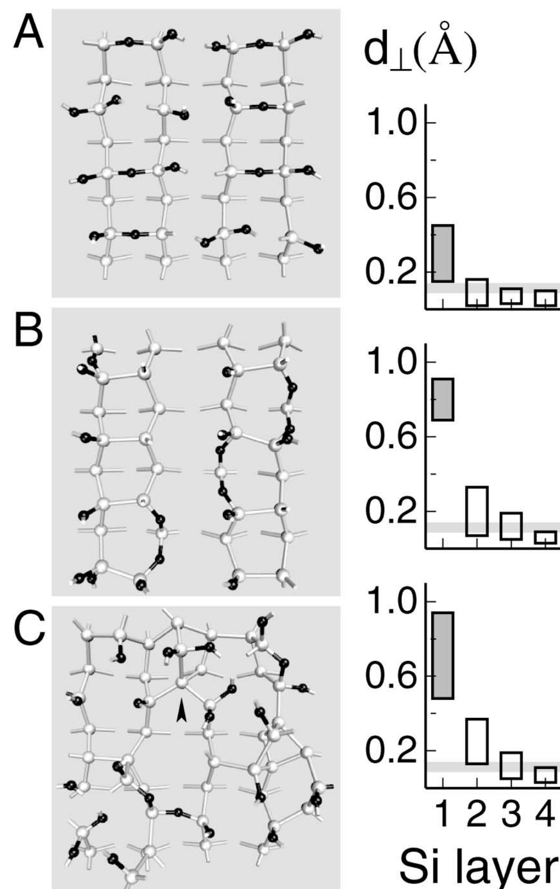

FIG. 2. Top views of transition structures in models *A*, *B*, and *C*. Light (dark) spheres indicate Si (O) atoms. Respective in-plane displacements for the upper 4 Si layers are given on the right. For each layer, a box is centered on the mean displacement with a vertical height giving the rms deviation. The first layer (dark box) contains partially oxidized Si atoms. The extra atom in model *C*, indicated by an arrow, was not considered as part of the substrate. The horizontal band indicates the sensitivity of ion-scattering measurements to atomic displacements.

either directly attached to the Si^{+1} moieties or located higher in the oxide. In model *B*, the terminating Si layer shows a high density of *in-plane* Si-Si dimers. To match the experimental suboxide distribution [9], we introduced O atoms in four of the backbonds of these dimers. The Si^{+1} and Si^{+2} moieties are distributed in the upper two layers of the substrate, while the Si^{+3} are partially in the terminating Si layer and partially higher in the oxide. In model *C*, the structure of the terminating Si layer was inspired by a model generated previously by first-principles molecular dynamics [13]. The occurrence of several in-plane Si-Si dimers and their disordered arrangement give rise to a transition region of two monolayers which contains most of the partially oxidized Si atoms (Fig. 2). Additional Si^{+3} moieties are found higher in the oxide. Model *C* also contains an extra Si atom with respect to a crystalline monolayer. This atom is in a Si^0

state and falls in the middle of the transition region (Fig. 2) [13].

We performed ion-scattering simulations on our model structures following the scheme used by Barrett [22], in which the interactions are described by Molière potentials. The thermal motion was accounted for by displacing atoms independently and randomly according to a Gaussian distribution [18,23]. For each thermal configuration, the yield was obtained in two steps. First, backscattering trajectories were identified by a steepest ascent procedure which searched for the maximal scattering angle. Then, the region around the identified trajectories was uniformly sampled. We used an acceptance aperture of 20°, sufficiently large to neglect effects occurring very close to the exit angle of 180° [24]. For the ideal Si column, we verified that this procedure reproduced documented results [18].

We assess the accuracy of the adopted simulation method by addressing Si(100) systems of known structure. For the clean Si(100)-(2×1) surface, a recent measurement with ion energies of 0.8 MeV found a Si yield of 13.4 ML [25], in agreement with our calculated yield of 13.1 ML. For the Si(100)-(1×1):H surface [26], theory and experiment [18] agree closely over an extended range of ion energies, showing a maximal error of 0.5 ML [Fig. 1(b)]. Hence, differences between experiment and simulation are not meaningful when smaller than $\sim$0.5 ML.

The ion-scattering simulations were designed to directly provide values for ΔY. Oxygen atoms and fully oxidized Si atoms were omitted from the outset in our simulation, to account for their statistically uniform distribution. Partially oxidized Si atoms, Si^{+x} with $x = 1, 2, 3$, were treated in the same way as nonoxidized Si atoms. To every Si^{+x}, we associated a number of O atoms equal to $x/2$, which was then accounted for in the calculation of ΔY, following the experimental definition of ΔY.

Excess Si yields were obtained by simulation for varying ion energies and are compared to measured values in Fig. 1. The calculated excess Si yields do not vary significantly with ion energy. We therefore averaged ΔY over ion energy, and obtained 3.0 ± 0.3 ML from our experimental data. This value should be compared with corresponding values of 1.4 ± 0.1, 2.7 ± 0.1, and 3.6 ± 0.2 ML obtained by simulation for models A, B, and C, respectively. This comparison indicates that the average yield for model A severely underestimates the experimental value, effectively ruling out model A as an acceptable structure for the Si(100)-SiO_2 interface. The yields for models B and C are both consistent with the experimental yields. Our results suggest that the bonding pattern at the Si(100)-SiO_2 interface is intermediate between those of models B and C.

The contribution to the excess Si yield from partially oxidized Si atoms, $\Delta Y^{\mathrm{subox}}$, is obtained under the well-justified assumption that these Si atoms do not interfere with the scattering at substrate columns. Accounting for the partial subtraction due to $Y_O/2$, we obtain $\Delta Y^{\mathrm{subox}} =$ 0.8 ML for the suboxide distributions in our models (Fig. 1). Data from different photoemission experiments give $\Delta Y^{\mathrm{subox}}$ differing from 0.8 ML by at most 0.15 ML [9,10]. The differences in the calculated ΔY for the three models originate solely from displacements of substrate Si atoms (Fig. 2). In model A, the O bridges cause significant displacements only in the first layer of the substrate leaving deeper ones unperturbed. In models B and C, important distortions propagate for several layers into the substrate.

To further understand the role of particular bonding configurations, we considered three other models, A', B', and C', derived by introducing minor variations with respect to their original counterparts. Model A' corresponds to an ideally abrupt interface, with the terminating Si layer consisting of Si^{+2} moieties bridged by O atoms and without any other intermediate oxidation state. Model B' differs from model A' by the terminating Si layer which consists of Si^{+1} moieties forming in-plane dimer bonds with each other. Model C' was obtained from the same surface template as for model C, with the omission of the extra Si atom [13].

For models A', B', and C', we obtained average excess Si yields of 0.9, 1.4, and 2.9 ML, respectively. These yields are compared in Fig. 3 to those of the previous models and to the experimental yield. Since the respective contributions $\Delta Y^{\mathrm{subox}}$ from intermediate oxidation states (0.75, 0.5, and 0.8 ML) do not vary significantly with respect to those of the previous models (0.8 ML), the variations in ΔY should mainly be assigned to different Si displacements. Models A and A' differ only by their suboxide distributions, and their yields are found to be close. The low yields calculated for models A' and B' show that ideally abrupt interfaces, either with O bridges or in-plane Si dimers in the terminating Si layer, are unable to account for the measured yield. The noticeable difference between the yields of models B' and B results from the oxidized backbonds in model B, which

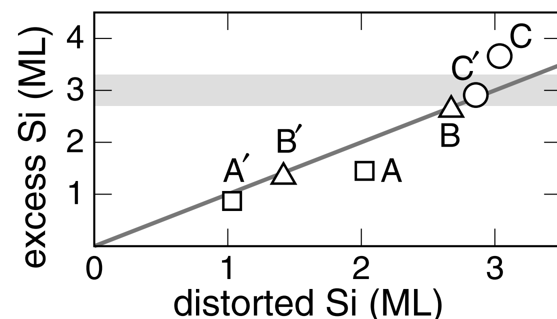

FIG. 3. Average excess Si yields for all model structures considered here vs number of Si atoms distorted by more than 0.09 Å. The horizontal band corresponds to the experimental result. The line is a guide to the eye.

significantly perturb the Si lattice. The decrease in yield from model C to model C' quantifies the effect of an extra Si atom in the transition region.

For each model, we quantifed the extent of Si displacements by counting the number of Si atoms of the substrate displaced from regular lattice sites by more than 0.09 Å, corresponding to the sensitivity of our ion-scattering experiment. The plot of excess Si yield vs the number of displaced Si atoms shows a nearly linear trend, indicating a close correlation. To reproduce the experimental yield of about 3 ML, the extent of the Si displacements should match those of models B and C. This level of distortion is achieved in these models by severely perturbing the terminating Si layer, either by backbond oxidation (model B) or by formation of a disordered bonding pattern (model C). Abruptly terminating Si substrates (models A' and B'), even when moderately perturbed to accommodate intermediate oxidation states (model A), do not present sufficiently large Si displacements.

In conclusion, from the interpretation of our experimental data, we infer that silicon distortions larger than 0.09 Å are found to propagate from the interface into the three upper layers of the Si lattice. These distortions are inconsistent with transition structures showing an ordered or nearly ordered pattern of O bridges [14,15], which could not be ruled out solely on the basis of photoemission data. This is because ion-scattering probes the silicon side of the interface, in contrast with photoemission which is mainly sensitive to the oxide side. The Si distortion reported here may affect electronic transport close to the interface and contribute to lowering the inversion-layer mobility as compared to its bulk value [27].

The authors thank Jochen Mullhaeuser for his contribution to the experimental part of this work. L. C. F. acknowledges useful discussions with C. R. Cirba and R. D. Schrimpf concerning electron transport at silicon interfaces. A. B. and A. P. acknowledge support from the Swiss National Science Foundation (Grants No. 21-55450.98 and No. 620-57850.99) and the Swiss Center for Scientific Computing. Support from DARPA and ONR (L. C. F.) is also acknowledged.

[1] L. C. Feldman, E. P. Gusev, and E. Garfunkel, in *Fundamental Aspects of Ultrathin Dielectrics on Si-Based Devices*, edited by E. Garfunkel *et al.* (Kluwer, Dordrecht, 1998), pp. 1–24.
[2] M. Schulz, Nature (London) **399**, 729 (1999).
[3] S. Tyagi *et al.*, Tech. Dig. Int. Electron Devices Meet. **2000**, 567 (2000).
[4] D. A. Muller *et al.*, Nature (London) **399**, 758 (1999).
[5] A. C. Diebold *et al.*, Mater. Sci. Semicond. Process. **2**, 103 (1999).
[6] N. Awaji *et al.*, Jpn. J. Appl. Phys. **35**, L67 (1996); S. D. Kosowsky *et al.*, Appl. Phys. Lett. **70**, 3119 (1997).
[7] S. C. Witczak, J. S. Suehle, and M. Gaitan, Solid-State Electron. **35**, 345 (1992).
[8] A. Stesmans and V. V. Afanas'ev, J. Phys. Condens. Matter **10**, L19 (1998).
[9] F. Rochet *et al.*, J. Non-Cryst. Solids **216**, 148 (1997); J. H. Oh *et al.*, Phys. Rev. B **63**, 205310 (2001).
[10] F. J. Himpsel *et al.*, Phys. Rev. B **38**, 6084 (1988); Z. H. Lu *et al.*, Appl. Phys. Lett. **63**, 2941 (1993).
[11] A. Pasquarello and Hybertsen, in *The Physics and Chemistry of SiO_2 and the Si-SiO_2 Interface–4*, edited by H. Z. Massoud *et al.* (Electrochemical Society, Pennington, 2000), p. 271.
[12] A. Pasquarello, M. S. Hybertsen, and R. Car, Phys. Rev. Lett. **74**, 1024 (1995); Phys. Rev. B **53**, 10 942 (1996).
[13] A. Pasquarello, M. S. Hybertsen, and R. Car, Nature (London) **396**, 58 (1998); in *Fundamental Aspects of Silicon Oxidation*, edited by Y. J. Chabal (Springer-Verlag, Berlin, 2001), p. 107.
[14] R. Buczko, S. J. Pennycook, and S. T. Pantelides, Phys. Rev. Lett. **84**, 943 (2000).
[15] Y. Tu and J. Tersoff, Phys. Rev. Lett. **84**, 4393 (2000); **89**, 086102 (2002).
[16] A. Pasquarello, M. S. Hybertsen, and R. Car, Appl. Phys. Lett. **68**, 625 (1996); Appl. Surf. Sci. **104/105**, 317 (1996); K.-O. Ng and D. Vanderbilt, Phys. Rev. B **59**, 10 132 (1999); A. A. Demkov and O. F. Sankey, Phys. Rev. Lett. **83**, 2038 (1999); T. Watanabe and I. Ohdomari, Thin Solid Films **343–344**, 370 (1999); T. Yamasaki *et al.*, Phys. Rev. B **63**, 115314 (2001).
[17] L. C. Feldman *et al.*, Phys. Rev. Lett. **41**, 1396 (1978); T. E. Jackman *et al.*, Surf. Sci. **100**, 35 (1980).
[18] I. Stensgaard, L. C. Feldman, and P. J. Silverman, Surf. Sci. **102**, 1 (1981); L. C. Feldman, J. W. Mayer, and S. T. Picraux, *Materials Analysis by Ion Channeling* (Academic Press, New York, 1982).
[19] A. Bongiorno and A. Pasquarello (unpublished).
[20] B. W. H. van Beest, G. J. Kramer, and R. A. van Santen, Phys. Rev. Lett. **64**, 1955 (1990).
[21] A. Pasquarello *et al.*, Phys. Rev. Lett. **69**, 1982 (1992); K. Laasonen *et al.*, Phys. Rev. B **47**, 10142 (1993). We described the electronic structure using an exchange-correlation energy functional, pseudopotentials, and plane-wave energy cutoffs, as in the first-principles calculations described in A. Bongiorno and A. Pasquarello, Phys. Rev. B **62**, R16 326 (2000).
[22] J. H. Barrett, Phys. Rev. B **3**, 1527 (1971).
[23] We adopted the experimental mean square displacement for Si at ambient temperature ($\langle u_x^2 \rangle^{1/2} = 0.075$ Å) [C. Flensburg and R. F. Stewart, Phys. Rev. B **60**, 284 (1999)]. Since this value lies close to the theoretical estimate of 0.081 Å for Si atoms in amorphous SiO_2 [A. Pasquarello, Phys. Rev. B **61**, 3951 (2000)], it is also expected to properly describe the partially oxidized Si atoms.
[24] P. P. Pronko *et al.*, Phys. Rev. Lett. **43**, 779 (1979).
[25] F. C. Stedile *et al.*, Nucl. Instrum. Methods Phys. Res., Sect. B **118**, 493 (1996).
[26] J. E. Northrup, Phys. Rev. B **44**, 1419 (1991).
[27] I. Polishchuk and C. Hu, in *Symposium on VLSI Circuits, Digest of Technical Papers, 2001* (Business Center for Academic Societies Japan, Tokyo, 2001), p. 51.